Desalination and Water Treatment
www.deswater.com

doi: 10.5004/dwt.2021.26883

219 (2021) 312–318
April

Collocation Trefftz method applied to groundwater tidal effect analysis

Yan Su[a,*], Luxi Yang[a,*], Lanqing Huang[a], Chengyu Ku[b]

[a]*Department of Water Resource and Harbor Engineering, College of Civil Engineering, Fuzhou University, Fuzhou 350108, China, emails: suyan@fzu.edu.cn (Y. Su), yanglx_959@outlook.com (L. Yang)*
[b]*Department of Harbor and River Engineering, National Taiwan Ocean University, Keelung 20224, China*

Received 15 August 2020; Accepted 23 November 2020

ABSTRACT

In coastal areas, tidal power causes periodic fluctuations of groundwater in coastal aquifers. In this paper, the response model of groundwater caused by tide is established by using the collocation Trefftz method (CTM) combined with the space–time coordinate system. Based on the governing equation of tidal response groundwater, the complete Trefftz basis of the equation is linearly superimposed, and the space–time coordinate system is combined to solve the variation of groundwater level with time and distance in the nearshore confined aquifer with tidal boundary. In this paper, the parameter sensitivity of numerical examples of CTM is analyzed by using analytical solution, and the parameter range of CTM to obtain highly accurate calculation results is discussed. In addition, this paper uses the CTM to analyze the tidal effect of groundwater, which has a strong practical significance for the application of this method to the study of coastal groundwater.

Keywords: Collocation Trefftz Method; Space–time coordinate system; Groundwater; Tidal; Parameter sensitivity

1. Introduction

Since 1950s, many researchers have conducted various studies on groundwater in coastal areas to explore related phenomena and problems. Jacob [1] used a one-dimensional analytical equation to describe the transmission of groundwater head fluctuations affected by tidal oscillations in coastal confined aquifers. This equation has also been widely used to evaluate actual data in many case studies. Sun [2] further extended the analytical solution to the two-dimensional groundwater problem. This type of problem considers head fluctuations in confined aquifers adjacent to the estuary, including changes in tidal amplitude and phase along the river bank. However, this solution cannot solve the effects of tides on the propagation of aquifers or the non-interacting tidal waves that exist on the coast. Taking into account the above situation, Jiao and Tang [3] proposed an analytical solution for describing the impact of tide on groundwater in coastal aquifers, but the interaction is too complicated to be predicted by Sun's solution. Li and Jiao [4] also studied an analytical solution to explore the influence of coastline shape on tidal head fluctuations, which can disregard the initial conditions of groundwater head distribution in coastal aquifers.

Since solving exact solutions of governing equations with different boundary conditions is a very complicated process, the analytical solutions proposed are usually solutions to simple problems solved under specific boundary conditions. Traditional numerical methods need to generate grids, and monotonous and tedious calculations can give an approximate solution to the problem [5], and collocation Trefftz method (CTM) is one of the most commonly used mesh-less methods that can quickly solve boundary value problems. At present, this method has been frequently used, and its approximate solution

* Corresponding authors.

can be expressed as a linear combination of functions that satisfy the governing equation [6]. According to the research of Kita et al. [7], Trefftz method is divided into direct method and indirect method. Li et al. [8,9] made a comprehensive comparison of the Trefftz method and other boundary methods, and concluded that the Trefftz method is the most convenient calculation method, which provides the most accurate equation solution and the best numerical stability. In order to obtain the exact solution of the linear equations, Ku et al. [10] proposed a generalized dynamic method based on the scalar homotopy method and proved the numerical stability of the Trefftz method for solving linear algebraic equations, especially for morbid problems. This method can obtain the solution of the system with extremely ill-conditioned conditions for the linear equations used in the three-dimensional Laplace problem. Recently, Ku et al. [11] also proposed a spatio-temporal mesh-less method to analyze transient groundwater flow in unsaturated porous media.

In this paper, CTM combined with the space–time coordinate system is used to solve the groundwater problems in the tidal zone. First, the Trefftz base of the tide response groundwater governing equation is combined with the spatiotemporal coordinate system to solve the change of groundwater amplitude of the near-shore confined aquifer at the tidal boundary with time and distance from the shore. Second, the analytical solution is used to analyze the parameter sensitivity of the numerical example of CTM. In addition, this paper also uses CTM to study the groundwater tidal effect.

2. Basic principle

Based on the homogeneous, uniform thickness and isotropic tidal response groundwater governing equation:

$$T\frac{\partial^2 h}{\partial x^2} - Lh = S\frac{\partial h}{\partial t} \tag{1}$$

where h is the head, t is the time, x is the distance from the shore, S is the storage coefficient of the aquifer, T is the transmissibility of the aquifer, and L is the leakage coefficient, where $L = k/b$, k and b, respectively, represent the vertical transmissibility and thickness of the impermeable layer.

The complete Trefftz basis that satisfies the governing equation is derived by the separation of variables, including the basis of groundwater in transient and steady states [12]. As follows:

$$h(x,t) = \left\{ \begin{matrix} e^{\left(\frac{Tp^2-L}{S}\right)t+px}, e^{\left(\frac{Tp^2-L}{S}\right)t-px}, e^{\sqrt{\frac{L}{T}}x}, e^{-\sqrt{\frac{L}{T}}x}, xe^{-\frac{L}{S}t}, \\ e^{-\frac{L}{S}t}, e^{-\left(\frac{Tp^2+L}{S}\right)t}\cos(px), e^{-\left(\frac{Tp^2+L}{S}\right)t}\sin(px) \end{matrix} \right\} \tag{2}$$

where p is the order of Trefftz basis.

The Trefftz basis is linearly superimposed by the superposition theorem, and the approximate solution of the governing equation for the Dirichlet boundary conditions is expressed as follows:

$$\begin{aligned} h(x,t) = {} & A_{01}e^{\sqrt{\frac{L}{T}}x} + B_{01}e^{-\sqrt{\frac{L}{T}}x} + A_{02}xe^{-\frac{L}{S}t} + B_{02}e^{-\frac{L}{S}t} \\ & + \sum_{p=1}^{w}\left[A_{1p}e^{\left(\frac{Tp^2-L}{S}\right)t+px} + B_{1p}e^{\left(\frac{Tp^2-L}{S}\right)t-px} \right] \\ & + \sum_{p=1}^{w}\left[A_{2p}e^{-\left(\frac{Tp^2+L}{S}\right)t}\cos(px) + B_{2p}e^{-\left(\frac{Tp^2+L}{S}\right)t}\sin(px) \right] \end{aligned} \tag{3}$$

where A_{01}, B_{01}, A_{02}, B_{02}, A_{1p}, B_{1p}, A_{2p}, B_{2p} are arbitrary constants, w is the order of the basis function suitable for the approximate solution of the governing equation.

Later, time and space are defined as independent variables based on the space–time coordinate system [13], and the space–time coordinate system is used to deal with the transient modeling of coastal aquifer groundwater. The two-dimensional coordinate system established in this paper includes one-dimensional time and one-dimensional space. The time and space boundaries are discretized into several points, and the head of the boundary satisfies the given conditions. The two-dimensional space–time coordinate system is used to solve the one-dimensional space groundwater problem (Fig. 1).

3. Numerical case

3.1. Parameter sensitivity analysis

In order to verify the influence of the number of boundary points (spatial boundary points, n_1, time boundary points, n_2) and order w on the accuracy of solving the groundwater level of the aquifer in one-dimensional coastal areas, the above parameters were set as variables to calculate the maximum absolute error of the groundwater head in the study area.

The study area is shown in Fig. 2, and the expression is as follows:

$$\Omega = \left\{ (x,t) 0 \le x \le L_n \right\} \tag{4}$$

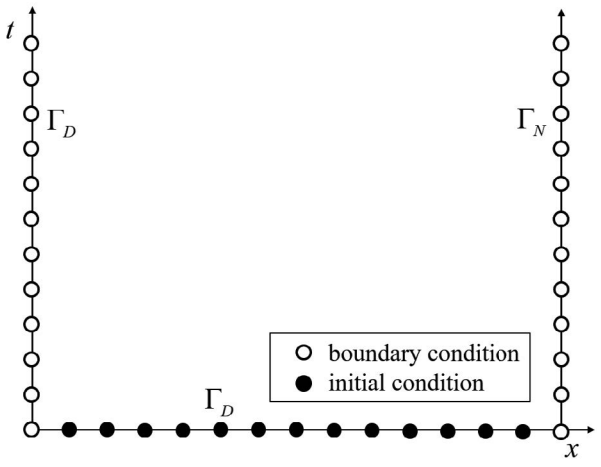

Fig. 1. Schematic diagram of space–time collocation.

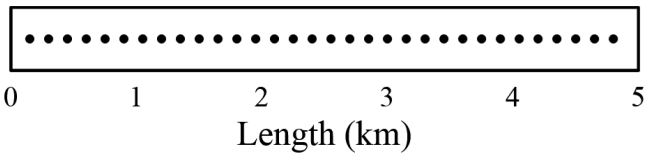

Fig. 2. Schematic diagram of the study area.

The analytical solution (38) to satisfy the tidal response groundwater governing equation is used as the boundary conditions and initial conditions of this case for parameter sensitivity analysis.

$$h(x,t) = -e^{\frac{-3L}{S}t}\cos\left(\sqrt{\frac{2L}{T}}x\right) + e^{-\left(\frac{L+T}{S}\right)}t\sin x \tag{5}$$

Calculate the maximum absolute error between the change of groundwater level in the coastal area of 1 km and the analytical solution (38) when the leakage coefficient is 0.12/d within 0–120 h. Where, in the process of analyzing the error of the number of boundary points, the transmissibility is 1,800 m^2/h, the storage coefficient is 2.0×10^{-4}, and the order is 25.

3.1.1. Error analysis of boundary points

Discrete the number of time boundary points into 50 points, and calculate the maximum absolute error when the number of space boundary points increases from 2 to 200. The results show that as the number of points on the space boundary increases, the maximum absolute error is basically stable and fluctuates between 10^{-14} and 10^{-15}. Especially, when the number of points is 24–27, the maximum absolute error broke through to 10^{-14}, it quickly dropped to 10^{-15}. In general, the change in the number of spatial boundary points has little effect on the calculation results, and the maximum absolute error is always maintained at a higher accuracy range lower than 10^{-13}

Similarly, discretize the number of space boundary points into 50 points, and calculate the maximum absolute error when the number of time boundary points increases from 2 to 200. The results show that the change of the maximum error with the number of time boundary points can be divided into four stages. In the first stage, when the number of points is 2 to 92, the maximum absolute error is stable around 10^{-15}, and as the number of points increases, there is a slight increase. In the second stage, when the number of points is between 93 and 109, the maximum absolute error linearly increases to 10^{-13} as the number of points increases. In the third stage, when the number of points is 110–124, the maximum absolute error is reduced from 10^{-13} and stabilized at 10^{-14}. In the fourth stage, when the number of points is between 125 and 200, due to the ill-conditioned nature of the matrix, as the number of points increases, the maximum absolute error increases significantly. Therefore, in the calculation process, the number of time boundary points should not be set too much while ensuring that the matrix avoids ill-conditioning.

3.1.2. Error analysis of order

In the process of order error analysis, the values of the transmissibility and storage coefficients are the same as those of the boundary point number error analysis, and the number of space–time boundary points is 50. Calculate the maximum absolute error when the order is increased from 1 to 100, and the result is shown in Fig. 3. It can be seen from the figure that when the order is increased from 1 to 7, the maximum absolute error is rapidly reduced from 10^{-3} to 10^{-15}. After the 7th order, as the order increases, although the maximum absolute error fluctuates to a certain extent, it is basically stable in the high-precision range between 10^{-13} and 10^{-15}. Therefore, in the calculation process, in order to ensure the calculation accuracy, the order should not be too low.

3.2. Analysis of tidal effect of groundwater

Amplitude attenuation and time lag are the unique tidal effect characteristics of groundwater in coastal areas. Therefore, the degree of groundwater tidal effect in coastal areas can be judged based on the tidal effect coefficient (TEC) and lag time, and the actual groundwater level in the aquifers in coastal areas can also be solved by using TEC and lag time to eliminate the influence of tidal fluctuations.

The groundwater amplitude shows a negative exponential decay trend with the increase of the distance from the shore, so the TEC is also defined as the ratio of the amplitude of the tidal fluctuation of confined groundwater (H_0) to the amplitude of the ocean tide (H_x) when the phase is the same [14].

$$\text{TEC} = \frac{H_0}{H_x} \tag{6}$$

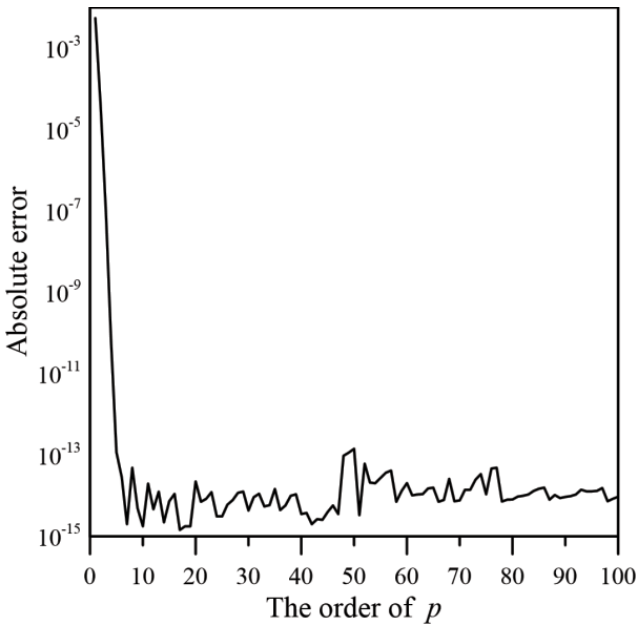

Fig. 3. Absolute error of order.

According to the phenomenon that groundwater exhibits a delay in propagation to the inland relative to tidal fluctuations, it is defined that the time it takes for tidal waves to pass from the coast to a certain point when flowing in aquifers is the lag time, which is represented by t_{lag} [14].

$$t_{lag} = t_G - t_T \tag{7}$$

When the tide is in the period of full-diurnal tide or semi-diurnal tide, in the aquifer system with different soil properties and leakage between different layers, the phenomena of amplitude attenuation and time delay also have different degrees of difference. By calculating the TEC and lag time, it is possible to compare and analyze the significant levels of groundwater tidal effects of different types of tides in different aquifer systems.

In the homogeneous and isotropic aquifer system in this case, the groundwater of the free aquifer leaks in the vertical direction through the impermeable aquifer and the confined aquifer. When the thickness of the free aquifer is sufficient, it can be effective. The ground restrains the influence of tides, so the groundwater fluctuations of the free aquifer are ignored, and the groundwater level of the free aquifer is parallel and equal to the sea level.

Within the study range of 3 km offshore (L_n) in coastal areas, the storage coefficient (S) is 5×10^{-4}, the total duration (t_{max}) is 6 h, and the tidal amplitude (A) is 1.5 m.

Based on the tidal response to the groundwater control Eq. (1), the tidal boundary condition (Γ_1) is generalized as sine function fluctuations [3].

$$h(0,t) = h_z + A\sin\left(\frac{2\pi}{t_0}t\right) \tag{8}$$

At a certain distance from the coast, when the inland water level is constant, the inland boundary (Γ_2) is expressed as follows:

$$h(x,t)\big|_{x=L_n} = 0 \tag{9}$$

Considering that the initial groundwater level is consistent with the average sea level, the initial conditions (Γ_3) are as follows:

$$h(x,t)\big|_{t=0} = 0 \tag{10}$$

The CTM considers arranging one source point and 903 boundary points uniformly distributed on the boundary on the space–time boundary. The specific number and order of collocation points are selected as shown in Table 1.

3.2.1. Influence of tide type on tide effect

Assume that two coastal areas with different tide types have the same transmissibility (T = 35 m²/h) and transmissibility (L = 0.005/d). Among them, the tide in the 1st area is a half-diurnal tide with a period of 12 h 25 min, that is, there are two high tides and two low tides in a day. The tide in the 2nd area is a full-diurnal tide with a period of 24 h 50 min, that is, there is only one high tide and one low tide in a day.

3.2.1.1. Effect of tide type on amplitude attenuation

It can be seen from Fig. 4 that the TEC shows an exponential decrease trend with the increase of the distance from the shore. When the tide belongs to the semi-diurnal tide type, the TEC decays slightly faster than the full-diurnal tide, that is, during the semi-diurnal tide period, coastal areas are affected by the tide. The phenomenon of attenuation of groundwater amplitude due to influence will be slightly more significant than the influence of all-day tide on groundwater.

According to Table 2, the width of the coastal area during the full-day tide is only 130 m wider than that during the half-day tide. Through exponential regression analysis, the TEC curve fitting equations of the two tide types are obtained. The two indices can directly reflect when the tide is in the whole day. During the tide or semi-diurnal tide period, with the change of the distance from the shore, the TEC differs little, which means that the type of tide has little effect on the attenuation of groundwater amplitude.

3.2.1.2. Effect of tide type on time lag

Different from the TEC, the influence degree of the fluctuation of the diurnal tide and the semi-diurnal tide on the delay of groundwater transfer is more obvious. The changes in the lag time of the two tidal periods in Fig. 5 all reflect that as the distance from the shore increases, the lag time of groundwater will be longer and longer, especially in

Table 1
Number of time–space boundary distribution points

	Space boundary point n_1	Time boundary point n_2	Order w	Internal point
Value	301	301	26	90,601
Spacing	10 m	0.1 h	–	–

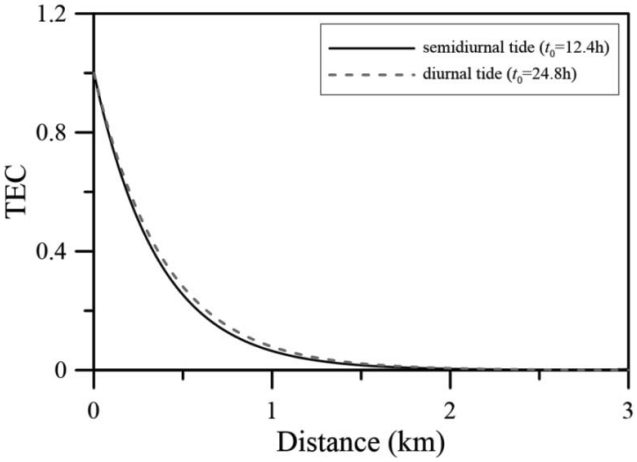

Fig. 4. Variation curve of tidal effect coefficient during full-diurnal and semi-diurnal tide.

Table 2
Results of tidal effect coefficient during the period of full-diurnal tide and half-diurnal tide

Tide type	Tide period t_0 (h)	Coastal area width (km)	TEC for change trend fitting equation
Half-diurnal tide	12.4	1.69	$y = e^{-2.5739x}$
All-day tide	24.8	1.82	$y = e^{-2.5481x}$

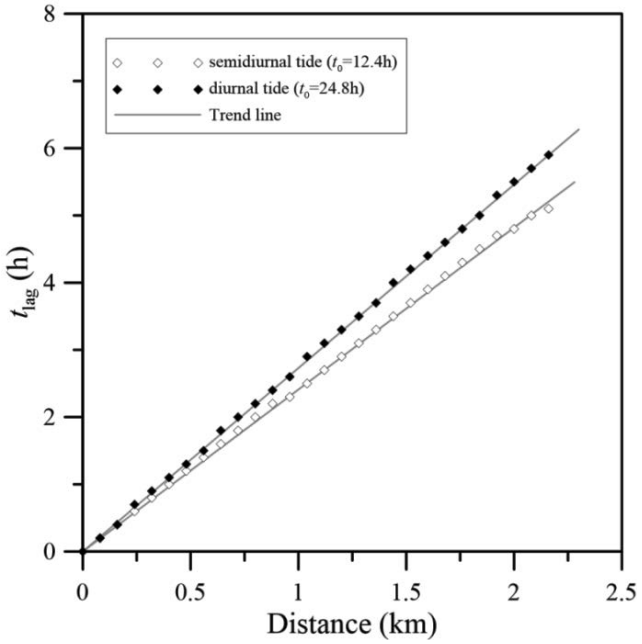

Fig. 5. Variation curve of lag time between diurnal tide and semi-diurnal tide.

coastal areas affected by the long-period full-day tide. Under the circumstances, the lag time is also longer.

From the equations of the lag time change trend in the two periods shown in Table 3 through linear regression analysis, it can be found that the slope of the diurnal tide is greater than that of the semidiurnal tide, which means that the offshore is getting farther and farther. The gap in the time lag of groundwater is also increasing.

3.2.2. Influence of soil properties on tidal effects

It is assumed that two coastal areas with different soil properties in aquifer systems belong to the all-diurnal tide with a tidal period (t_0 = 24.8 h). Among them, the 1st area is a sandy soil layer, and the 2nd area is a gravel layer.

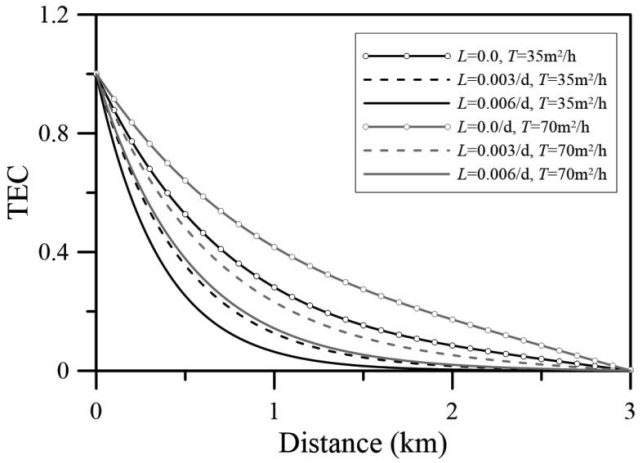

Fig. 6. Variation curve of tidal effect coefficient of sand layer and gravel layer.

The values of the transmissibility and the leakage coefficient are shown in Table 4.

3.2.2.1. Influence of soil properties on amplitude attenuation

The larger the transmissibility of the confined aquifer and the smaller the leakage coefficient, the greater the impact of tidal fluctuations on groundwater [14]. Fig. 6 clearly confirms this theory: in the case of the same leakage, the gravel layer with better permeability has greater groundwater amplitude than the sand layer with weaker permeability; while the same soil properties are under pressure in the aquifer, the increase in leakage will cause the groundwater amplitude to decay.

3.2.2.2. Effect of soil properties on time lag

According to Table 5, when the confined aquifer is a gravel layer, the range of the coastal area is larger than when the confined aquifer is a sand layer, and with the increase of leakage, the gap in the range of coastal areas becomes

Table 3
Results of the lag time during the day tide and half day tide

Tide type	Tide period t_0 (h)	t_{lag} for different distances from shore (h)				t_{lag} for change trend fitting equation
		0.5 km	1.0 km	1.5 km	2.0 km	
Half-diurnal tide	12.4	1.2	2.4	3.7	4.8	$y = 2.3976x$
All-day tide	24.8	1.4	2.8	4.1	5.5	$y = 2.7285x$

larger and larger. It can be proved that the permeability and leakage of aquifer soil in coastal areas have a combined effect on the amplitude of groundwater fluctuations.

It can be seen from Fig. 7 that due to the impact of tidal fluctuations in coastal areas, in aquifers with any soil properties and any leakage amount, the lag time of groundwater increases linearly with the increase of the distance from the shore. When the leakage in the aquifer system is larger, the soil with better permeability is, and the lag time of groundwater is shorter.

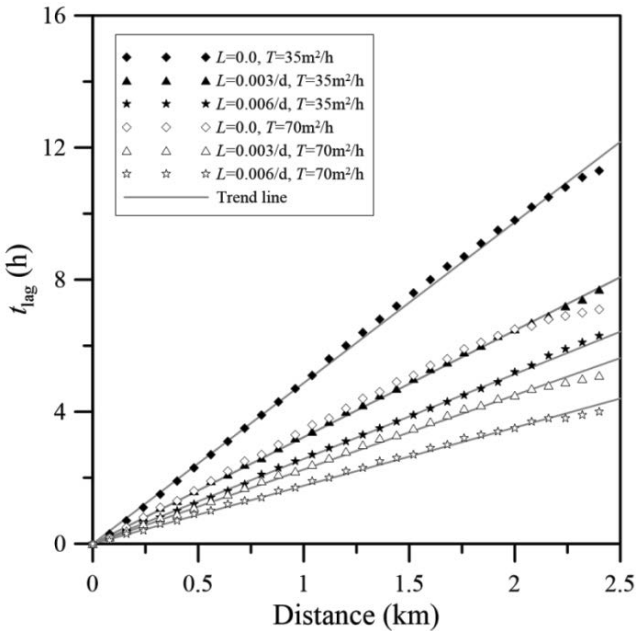

Fig. 7. Variation curve of lag time between sand layer and gravel layer.

The equation of the lag time change trend is obtained by linear regression analysis and fitting. As shown in Table 6, it is found that in aquifer systems with low leakage and weaker permeability, the linear growth rate of groundwater lag time is faster, which means it is also more affected by tidal fluctuations.

4. Conclusions

This paper, by using the Trefftz basis of the governing equation of tide-induced groundwater and the space–time coordinate system, carries out the parameter sensitivity analysis and tidal groundwater effect analysis. This paper simulates two numerical examples to study the feasibility and accuracy of CTM and the coastal aquifer.

Table 4
Aquifer soil properties and values of various parameters

Aquifer soil properties	Transmissibility T (m²/h)	Leakage coefficient L (/d)
Sand layer	35	0.0
Gravel layer	70	0.003 0.006

Table 5
Results of tidal effect coefficients for sand and gravel layers at different leakage

Leakage coefficient L (1/d)	Transmissibility T (m²/h)	Coastal area width (km)	TEC for change trend fitting equation
0.0	35	2.88	$y = e^{-1.3576x}$
	70	2.95	$y = e^{-1.0434x}$
0.003	35	2.23	$y = e^{-2.1241x}$
	70	2.76	$y = e^{-1.5735x}$
0.006	35	1.68	$y = e^{-2.6589x}$
	70	2.34	$y = e^{-2.0319x}$

Table 6
Results of lag time for sand and gravel layers at different leakage

Leakage coefficient L (d)	Transmissibility T (m²/h)	t_{lag} for different distances from shore (h)				t_{lag} for change trend fitting equation
		0.5 km	1.0 km	1.5 km	2.0 km	
0.0	35	2.4	4.9	7.5	9.8	$y = 4.866x$
	70	1.7	3.4	5.1	6.5	$y = 3.2272x$
0.003	35	1.7	3.3	4.9	6.5	$y = 3.230x$
	70	1.2	2.3	3.5	4.5	$y = 2.5543x$
0.006	35	1.3	2.6	3.8	5.2	$y = 2.25735x$
	70	0.9	1.8	2.7	3.5	$y = 1.7556x$

By changing the boundary points number and order of space–time, the example of parameter sensitivity analysis provides the optimal parameter value range, which can avoid the ill-conditioned matrix and ensure the accuracy of CTM.

Through the calculation of the coefficient of tidal effect and lag time, the example of groundwater tidal effect analysis shows that the tide type has little effect on the attenuation of groundwater amplitude, but has a significant delay effect on the transfer time of groundwater. In addition, the example also proves that better the permeability, larger the groundwater amplitude, shorter the lag time, and more the leakage, worse the groundwater amplitude attenuation.

This paper discusses the discovery and contribution of CTM. It is suggested that the groundwater problem about multi-dimensional space and complex soils can be developed in the future, and the mutual interaction between various aquifers can be comprehensively considered, which will greatly improve the applicability of this method to coastal engineering groundwater research.

References

[1] C.E. Jacob, Flow of Groundwater, H. Rouse, Ed., Engineering Hydraulics, John Wiley, New York, 1950, pp. 321–386.
[2] H. Sun, A two-dimensional analytical solution of groundwater response to tidal loading in an estuary, Water Resour. Res., 33 (1997) 1429–1435.
[3] J.J. Jiao, Z. Tang, An analytical solution of groundwater response to tidal fluctuation in a leaky confined aquifer, Water Resour. Res., 35 (1999) 747–751.
[4] H. Li, J.J. Jiao, Tidal groundwater level fluctuations in L-shaped leaky coastal aquifer system, J. Hydrol., 268 (2002) 234–243.
[5] C.Y. Liu, C.Y. Ku, J.E. Xiao, W. Yeih, A novel spacetime collocation meshless method for solving two-dimensional backward heat conduction problems, Comp. Model. Eng. Sci., 118 (2019) 229–252.
[6] E. Trefftz, E. Gegenstuck zum, R. Verfahren, Proceedings of the 2nd International Congress for Applied Mechanics, Zurich, Switzerland, 1926, pp. 131–137.
[7] E. Kita, N. Kamiya, Trefftz method: an overview, Adv. Eng. Softw., 24 (1995) 3–12.
[8] Z.C. Li, T.T. Lu, H.T. Huang, A.H.D. Cheng, Trefftz collocation, and other boundary methods—a comparison, Numer. Methods Partial Differ. Equations, 23 (2007) 93–144.
[9] Z.C. Li, T.T. Lu, H.Y. Hu, A.H.D. Cheng, Trefftz and Collocation Methods, Southampton, WIT Press, Boston, 2008.
[10] C.Y. Ku, W. Yeih, C.S. Liu, Dynamical Newton-like methods for solving Ill-conditioned systems of nonlinear equations with applications to boundary value problems, Comput. Model Eng. Sci., 76 (2011) 83–108.
[11] C.-Y. Ku, C.-Y. Liu, Y. Su, J.-E. Xiao, Modeling of transient flow in unsaturated geomaterials for rainfall-induced landslides using a novel spacetime collocation method, Geofluids, 2018 (2018) 1–16.
[12] C.Y. Ku, C.Y. Liu, Y. Su, L. Yang, W.P. Huang, Modeling tide-induced groundwater response in a coastal confined aquifer using the space-time collocation approach, Appl. Sci., 10 (2020) 439.
[13] C.Y. Ku, C.Y. Liu, W. Yeih, C.S. Liu, C.M. Fan, A novel space-time meshless method for solving the backward heat conduction problem, Int. J. Heat Mass Transf., 130 (2019) 109–122.
[14] J.G. Ferris, Cyclic Water-Level Fluctuations as a Basis for Determining Aquifer Transmissibility, In: R. Bentall, Ed., Methods of Determining Permeability, Transmissibility and Drawdown, Washington, DC, pp. 305–318.